2-1-2008

Organization and Instabilities of Entangled Active Polar Filaments

Tanniemola B. Liverpool
Imperial College and University of California

M. Cristina Marchetti
Syracuse University and University of California

Recommended Citation

arXiv:cond-mat/0207320v1

Organization and instabilities of entangled active polar filaments.

Tanniemola B. Liverpool[1,3] and M. Cristina Marchetti[2,3]
[1] *Condensed Matter Theory Group, Blackett Laboratory, Imperial College, London, SW7 2BW*
[2] *Physics Department, Syracuse University, Syracuse, NY 13244*
[3] *Kavli Institute of Theoretical Physics, University of California, Santa Barbara, CA 93106*
(Dated: February 1, 2008)

We study the dynamics of an entangled, isotropic solution of polar filaments coupled by molecular motors which generate relative motion of the filaments in two and three dimensions. We investigate the stability of the homogeneous state for constant motor concentration taking into account excluded volume and entanglement. At low filament density the system develops a *density* instability, while at high filament density entanglement effects drive the instability of *orientational* fluctuations.

PACS numbers: 87.16.-b,47.54.+r,05.65.+b

Cellular biology provides many realizations of pattern formation in dissipative nonequilibrium systems. An important example is the collective behavior of the proteins that compose the cytoskeleton of eukaryotic cells. The cytoskeleton provides both the supporting structure of the cell and the vehicle for internal transport processes [1]. It is a network of long protein filaments, mainly microtubules, actin filaments and intermediate filaments, coupled by smaller proteins, such as molecular motors and cross-linkers. Motor proteins convert chemical energy derived from the hydrolysis of ATP (Adenosine TriPhosphate) into mechanical work, generating forces and motion of the filaments relative to each other in these *active gels*.

Numerous *in vitro* experiments [2, 3, 4, 5] have shown that mixtures of filaments and their associated motor proteins self-organize into macroscopic symmetry-breaking structures, including radial arrays or asters and one-dimensional bundles. The nonequilibrium forces that give rise to these structures include the action of molecular motors and the polymerization/depolymerization process of the filaments [7]. Here we focus on the role of motor proteins and assume that the filaments have fixed length — a situation that can be achieved in vitro [4]. A few analytical and numerical studies have investigated the emergence of these complex patterns [4, 5, 8, 9, 10, 11, 12]. Continuum models of filament/motor systems in two dimensions have been used to show that spatial patterns are obtained as nonequilibrium solutions of the system dynamics [9, 11]. These models have ignored either filament diffusion [11] or the motor action on orientational dynamics [9]. A more microscopic approach was taken by Kruse *et al* who considered a dynamical model for the development of contractile and motile structures in *one dimensional* polar filament bundles, while ignoring steric and other interactions between the filaments [10, 12].

Many open questions remain concerning the role of the physical properties of the filament/motor gel in controlling the formation of self-organized structures. Experiments have indicated that motor properties, such as their processivity – the fraction of time in a cycle a motor remains attached to the filament, strongly influence pattern formation. This is evident by comparing *in vitro* experiments in microtubules-kinesin to those in actin-myosin mixtures. At high motor concentration, microtubule-kinesin mixtures readily organize in a variety of spatial patterns, provided the motors stall at the polymer ends before detaching [4, 5]. In contrast, the homogeneous state is much more robust in the weakly coupled actin-myosin II systems, where spatially inhomogeneous structures develop only upon depletion of ATP or at much higher filament concentration [13]. The physical characteristics of the filaments, such as their persistence length, may also contribute to the different behavior of these two active gels, as actin-myosin networks are more strongly entangled than microtubule-kinesin mixtures. Both analytic theories [10, 11, 12] and simulations [4, 5] have so far entirely *neglected* entanglement.

In this letter we start from a phenomenological model in the spirit of Kruse et al. [10, 12] and obtain a set of continuum equations to describe the dynamics and organization of polar filaments driven by molecular motors in an unconfined geometry in (quasi-)two and three dimensions ($d = 2, 3$). By modeling the motor-filament interaction microscopically, we can calculate the magnitude and, most importantly, the sign of the parameters of the continuum equations, which cannot be obtained by symmetry arguments. We consider a isotropic filament solution and include the effects of *entanglement* and *excluded volume*. Our result is a phase diagram (Fig. 2) as a function of the filament density and motor properties.

The filaments are modeled as rigid rods of length l and diameter $b << l$. Each filament is identified by the position $\mathbf{r}$ of its center of mass and a unit vector $\hat{\mathbf{n}}$ pointing towards the polar end. Taking into account *filament transport*, the normalized filament probability distribution function, $\Psi(\mathbf{r}, \hat{\mathbf{n}}, t)$, obeys a conservation law [14],

$$\partial_t \Psi + \nabla \cdot \mathbf{J} + \mathcal{R} \cdot \mathbf{J}^{\mathbf{r}} = \mathbf{0} \,, \tag{1}$$

where $\mathcal{R} = \hat{\mathbf{n}} \times \partial_{\hat{\mathbf{n}}}$ is the rotation operator. The transla-

tional and rotational currents $\mathbf{J}$ and $\mathbf{J^r}$ are given by

$$J_i = -D_{ij}\partial_j\Psi - \frac{D_{ij}}{k_BT}\ \Psi\ \partial_j V_{\rm ex} + J_i^{\rm act}\ , \qquad (2)$$

$$J_i^r = -D_r\mathcal{R}_i\Psi - \frac{D_r}{k_BT}\ \Psi\ \mathcal{R}_i V_{\rm ex} + J_i^{\rm r/act}\ , \qquad (3)$$

where $i = 1, ..., d$ and $D_{ij} = D_\parallel \hat{n}_i\hat{n}_j + D_\perp(\delta_{ij} - \hat{n}_i\hat{n}_j)$ is the translational diffusion tensor and D_r the rotational diffusion constant. The potential $V_{\rm ex}$ incorporates excluded volume effects that play an important role in stabilizing time-dependent solutions. It is given by k_BT times the probability of finding another rod in the interaction area of a given rod,

$$V_{\rm ex}(\mathbf{r}, \hat{\mathbf{n}}_1) = k_BT \int_{\hat{\mathbf{n}}_2}\int_{\boldsymbol{\xi}}{}' \Psi(\mathbf{r}+\boldsymbol{\xi}, \hat{\mathbf{n}}_2)\ , \qquad (4)$$

where the prime restricts the integral to the interaction volume, corresponding to the region where the two filaments touch at at least one point. The volume of this region is $V_{\rm int} = v_0\sqrt{1-(\hat{\mathbf{n}}_1\cdot\hat{\mathbf{n}}_2)^2}$, with $v_0 = l^2b^{d-2}$ and $l^2\sqrt{1-(\hat{\mathbf{n}}_1\cdot\hat{\mathbf{n}}_2)^2} > b^2$. The active currents are given by

$$\mathbf{J}^{\rm act}(\mathbf{r}, \hat{\mathbf{n}}_1) = \int_{\hat{\mathbf{n}}_2}\int_{\boldsymbol{\xi}}{}' \mathbf{v}(\boldsymbol{\xi}, \hat{\mathbf{n}}_1, \hat{\mathbf{n}}_2)\Psi(\mathbf{r}, \hat{\mathbf{n}}_1)\Psi(\mathbf{r}+\boldsymbol{\xi}, \hat{\mathbf{n}}_2), \qquad (5)$$

$$\mathbf{J}^{\rm r/act}(\mathbf{r}, \hat{\mathbf{n}}_1) = \int_{\hat{\mathbf{n}}_2}\int_{\boldsymbol{\xi}}{}' \boldsymbol{\omega}(\boldsymbol{\xi}, \hat{\mathbf{n}}_1, \hat{\mathbf{n}}_2)\Psi(\mathbf{r}, \hat{\mathbf{n}}_1)\Psi(\mathbf{r}+\boldsymbol{\xi}, \hat{\mathbf{n}}_2), \qquad (6)$$

where $\mathbf{v} = -\dot{\boldsymbol{\xi}}$ and $\boldsymbol{\omega} = \dot{\hat{\mathbf{n}}}_1 - \dot{\hat{\mathbf{n}}}_2$ are the relative linear and angular velocities of two filaments, with the dot denoting a time derivative. The model naturally contains two competing dynamics. The first is the diffusion of hard rods, which at high density must include excluded volume and entanglement. The second is the local driving force coming from the interaction with the motors. This depends on the polarity of the filaments and breaks the $\hat{\mathbf{n}} \to -\hat{\mathbf{n}}$ symmetry of the hard rod fluid, allowing for states of broken symmetry, where the filaments acquire a nonvanishing mean orientation.

In the absence of external forces and torques the total linear and angular velocity of an interacting pair are conserved. This requires $\mathbf{v}(\boldsymbol{\xi}, \hat{\mathbf{n}}_1, \hat{\mathbf{n}}_2) = -\mathbf{v}(-\boldsymbol{\xi}, \hat{\mathbf{n}}_1, \hat{\mathbf{n}}_2)$ and $\boldsymbol{\omega}(\boldsymbol{\xi}, \hat{\mathbf{n}}_1, \hat{\mathbf{n}}_2) = -\boldsymbol{\omega}(-\boldsymbol{\xi}, \hat{\mathbf{n}}_1, \hat{\mathbf{n}}_2)$. Rotational and translational invariance requires $\mathbf{v}(\boldsymbol{\xi}, \hat{\mathbf{n}}_1, \hat{\mathbf{n}}_2) = -\mathbf{v}(-\boldsymbol{\xi}, -\hat{\mathbf{n}}_1, -\hat{\mathbf{n}}_2)$ and $\boldsymbol{\omega}(\boldsymbol{\xi}, \hat{\mathbf{n}}_1, \hat{\mathbf{n}}_2) = \boldsymbol{\omega}(-\boldsymbol{\xi}, -\hat{\mathbf{n}}_1, -\hat{\mathbf{n}}_2)$. The simplest form of the linear and angular velocities can be written as

$$\mathbf{v} = \frac{\alpha}{2l}\ \frac{\boldsymbol{\xi}(1+\hat{\mathbf{n}}_1\cdot\hat{\mathbf{n}}_2)}{\sqrt{1-(\hat{\mathbf{n}}_1\cdot\hat{\mathbf{n}}_2)^2}} + \frac{\beta}{2}\frac{\hat{\mathbf{n}}_2-\hat{\mathbf{n}}_1}{\sqrt{1-(\hat{\mathbf{n}}_1\cdot\hat{\mathbf{n}}_2)^2}}\ , \qquad (7)$$

$$\boldsymbol{\omega} = \gamma\ (\hat{\mathbf{n}}_1\cdot\hat{\mathbf{n}}_2)\ \frac{\hat{\mathbf{n}}_1\times\hat{\mathbf{n}}_2}{\sqrt{1-(\hat{\mathbf{n}}_1\cdot\hat{\mathbf{n}}_2)^2}}\ . \qquad (8)$$

The velocities have been normalized with the volume of interaction. The parameters α, β and γ are the rates for the various motor-induced translations and rotations

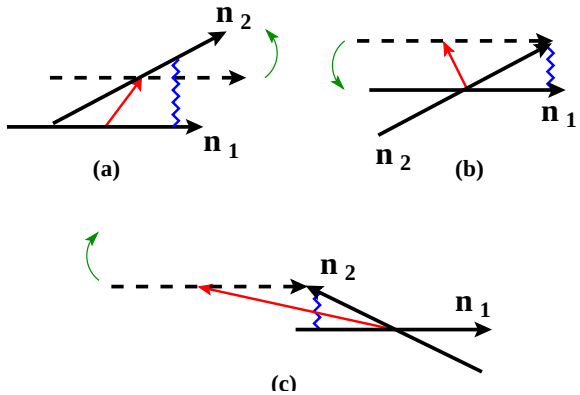

FIG. 1: Cartoons of various motor-induced filament interactions. All interactions are viewed from the rest frame of filament 2. The initial and final position of filament 1 are shown as a thick and a dashed arrow, respectively. The zigzaged lines represent motors. (a) The contribution to $\mathbf{v}$ proportional to α which is along the direction of the relative displacement $\boldsymbol{\xi}$ of the centers of mass of the two filaments (thin arrow). Motors also drive rotation of filament 1 as indicated. The contribution to $\mathbf{v}$ proportional to β is illustrated in (b) and (c) for two filaments with $\boldsymbol{\xi} = 0$ and $\hat{\mathbf{n}}_1\cdot\hat{\mathbf{n}}_2 > 0$ (b) and $\hat{\mathbf{n}}_1\cdot\hat{\mathbf{n}}_2 < 0$ (c). In both cases the translation at a rate β in the direction of $\hat{\mathbf{n}}_2 - \hat{\mathbf{n}}_1$ (thin arrow) tends to bring the polar heads of the two filaments to the same spatial location. In (b) the counterclockwise rotation aligns the filaments, while in (c) the clockwise rotation anti-aligns and separates.

(Fig. 1). The contribution proportional to α depends on the separation of the centers of the filaments and results from a difference in motor activity between the ends and mid-points of the filaments. It tends to align the centers of mass and polar heads of the filament pair (see Fig 2(a)). The contribution proportional to β vanishes for aligned filaments and can separate antiparallel filaments, as illustrated in Fig. 2(c). This mechanism yields both translational and rotational currents. The prefactor $(\hat{\mathbf{n}}_1\cdot\hat{\mathbf{n}}_2)$ in the angular velocity guarantees that motors preferentially bind to two filaments that are at an angle smaller than $\pi/2$. The γ term has no effect on perpendicular filaments. Assuming uniform motor density ρ_m, from simple mechanical models of motors [1], we estimate $\alpha \simeq \beta \simeq \gamma l \simeq \rho_m l b^2 \phi(s_c/\tau_c)$, with s_c the motor step length per cycle, τ_c the time for one cycle and ϕ the duty ratio.

We are interested in describing the dynamics of active filaments on length scales large compared to the filaments size, l. We can then expand the concentration of filaments $\Psi(\mathbf{r}+\boldsymbol{\xi}, \hat{\mathbf{n}}_2)$ near its value at $\mathbf{r}$,

$$\Psi(\mathbf{r}+\boldsymbol{\xi}, \hat{\mathbf{n}}_2) = \Psi(\mathbf{r}, \hat{\mathbf{n}}_2) + \xi_n\hat{\mathbf{e}}_n\cdot\nabla\Psi(\mathbf{r}, \hat{\mathbf{n}}_2) + \frac{1}{2}\xi_n\xi_m(\hat{\mathbf{e}}_n\cdot\nabla)(\hat{\mathbf{e}}_m\cdot\nabla)\Psi(\mathbf{r}, \hat{\mathbf{n}}_2) + O(\xi^3). \qquad (9)$$

We have introduced a set of orthogonal unit vectors, $(\hat{\mathbf{e}}_1, \hat{\mathbf{e}}_2, \hat{\mathbf{z}})$, that provides a natural coordinate system for the problem. The unit vector $\hat{\mathbf{z}}$ is normal to the plane

passing through the point of contact of the two filaments and containing the unit vectors $\hat{\mathbf{n}}_1$ and $\hat{\mathbf{n}}_2$. The vectors $\hat{\mathbf{e}}_1 = (\hat{\mathbf{n}}_1 + \hat{\mathbf{n}}_2)/|\hat{\mathbf{n}}_1 + \hat{\mathbf{n}}_2|$ and $\hat{\mathbf{e}}_2 = \mathrm{sign}\big(\hat{\mathbf{n}}_1 \cdot \hat{\mathbf{n}}_2\big)(\hat{\mathbf{n}}_2 - \hat{\mathbf{n}}_1)/|\hat{\mathbf{n}}_2 - \hat{\mathbf{n}}_1|$ are orthogonal unit vectors in this plane. Neglecting the out-of-plane separation (of order b) between the centers of mass of the two filaments, the vector $\boldsymbol{\xi}$ is written in this coordinate system as $\boldsymbol{\xi} = \xi_n \hat{\mathbf{e}}_n$, where summation over $n = 1, 2$ is intended. We assume that on large scales the filament dynamics can be described in terms of the filaments density $\rho(\mathbf{r})$ and the local filament orientation $\mathbf{t}(\mathbf{r})$ defined as the first two moments of the distribution $\Psi(\mathbf{r}, \hat{\mathbf{n}}, t)$,

$$\begin{pmatrix} \rho(\mathbf{r},t) \\ \mathbf{t}(\mathbf{r},t) \end{pmatrix} = \int d\hat{\mathbf{n}} \begin{pmatrix} 1 \\ \hat{\mathbf{n}} \end{pmatrix} \Psi(\mathbf{r}, \hat{\mathbf{n}}, t) \; . \tag{10}$$

Coarse-grained equations for ρ and $\mathbf{t}$ can be obtained by inserting Eq. (9) in the expressions for the active currents and for $V_{\rm ex}$, writing the density $\Psi(\mathbf{r}, \hat{\mathbf{n}}, t)$ in the form of an exact moment expansion, and retaining only the first two moments in this expansion. For brevity, we only display here the dynamical equations linearized about a homogeneous state, with constant density ρ_0 and an isotropic orientational distribution of filaments, corresponding to $\mathbf{t} = 0$. The full and rather cumbersome nonlinear equations will be given elsewhere [15]. Letting $\rho = \rho_0 + \delta\rho$ and keeping only terms up to third order in the gradients, the linearized equations are given by

$$\partial_t \delta\rho = \frac{1}{d}\big[D_\parallel + (d-1)D_\perp\big](1 + v_0\rho_0)\nabla^2\delta\rho - \frac{\alpha l v_0 \rho_0}{12d}\nabla^2\delta\rho - \frac{\beta l^2 v_0 \rho_0 (2d+1)}{24d(d+2)}\nabla^2(\boldsymbol{\nabla}\cdot\mathbf{t}) \; , \tag{11}$$

$$\begin{aligned} \partial_t t_i \;=\; & -D_r t_i + \frac{1}{d+2}\big[(d+1)D_\perp + D_\parallel\big]\nabla^2 t_i + \frac{2}{d+2}\big(D_\parallel - D_\perp\big)\partial_i \nabla\cdot\mathbf{t} \\ & - \frac{\alpha l v_0 \rho_0}{12d(d+2)}\big[\nabla^2 t_i + 2\partial_i \boldsymbol{\nabla}\cdot\mathbf{t}\big] + \frac{\beta v_0 \rho_0}{d}\partial_i\delta\rho + \frac{\beta l^2 v_0 \rho_0 (2d+1)}{24 d^2 (d+2)}\partial_i\nabla^2\delta\rho \; . \end{aligned} \tag{12}$$

The local orientation is not a conserved variable and decays at a rate $\sim D_r$. Both equations display the competition of diffusive terms ($\propto D\nabla^2$) and pattern-forming terms ($\propto -\alpha\nabla^2$). The linear instability of the homogeneous state occurs when the pattern-forming terms dominate. To linear order, the contribution from the rotational current vanishes and excluded volume corrections only appear in the density equation.

We now study the stability of the homogeneous state. We expand the fields in Fourier components, $\delta\rho(\mathbf{r}) = \sum_{\mathbf{k}} \rho_{\mathbf{k}} e^{i\mathbf{k}\cdot\mathbf{r}}$ and $\mathbf{t}(\mathbf{r}) = \sum_{\mathbf{k}} \mathbf{t}_{\mathbf{k}} e^{i\mathbf{k}\cdot\mathbf{r}}$, and separate $\mathbf{t}_{\mathbf{k}}$ in its component longitudinal and transverse to $\mathbf{k}$, namely $t^L_{\mathbf{k}} = \hat{\mathbf{k}}\cdot\mathbf{t}_{\mathbf{k}}$ and $t^T_{\mathbf{k}} = \hat{\mathbf{k}}\times\mathbf{t}_{\mathbf{k}}$, with $\hat{\mathbf{k}} = \mathbf{k}/|\mathbf{k}|$. In d dimensions there are $d-1$ degenerate transverse modes describing the decay of fluctuations in $t^T_{\mathbf{k}}$, with rate

$$\lambda_T(k) = -D_r - \frac{k^2}{d+2}\Big[(d+1)D_\perp + D_\parallel - \frac{\alpha l v_0 \rho_0}{12d}\Big] \; . \tag{13}$$

There are two coupled modes describing the decay of density and $t^L_{\mathbf{k}}$ fluctuations, given by

$$\lambda_\pm(k) = \frac{1}{2}\Big\{M_{11} + M_{22} \pm \sqrt{(M_{11}-M_{22})^2 + 4M_{12}M_{21}}\Big\} \; , \tag{14}$$

with

$$\begin{aligned} M_{11} &= -\frac{k^2}{d}\Big[(D_\parallel + (d-1)D_\perp)(1+v_0\rho_0) - \frac{\alpha l v_0\rho_0}{12}\Big] \; , \\ M_{22} &= -D_r - \frac{k^2}{d+2}\Big[3D_\parallel + (d-1)D_\perp - \frac{\alpha l v_0\rho_0}{4d}\Big] \; , \\ M_{12} &= ik^3 \frac{\beta l^2 v_0\rho_0}{24}\frac{2d+1}{d(d+2)} \; , \\ M_{21} &= ik\frac{\beta v_0\rho_0}{d}\Big(1 - \frac{l^2k^2}{24}\frac{2d+1}{d(d+2)}\Big) \; . \end{aligned} \tag{15}$$

At long wavelength, $\lambda_+ \equiv \lambda_\rho$ vanishes as k^2 and describes the decay of density fluctuations, while $\lambda_- \equiv \lambda_L$ is a kinetic mode (i.e., it is finite as $k \to 0$) and describes the decay of longitudinal orientation fluctuations. The hydrodynamic density mode goes unstable on all length scales for $\tilde{\alpha} > \tilde{\alpha}^{(1)}_c \simeq (1 + (d-1)D_\perp/D_\parallel)[1 + (\tilde{\rho}_0)^{-1}]$, where $\tilde{\alpha} = \alpha l/(12 D_\parallel)$ and $\tilde{\rho}_0 = \rho_0 v_0$.

Dilute Solutions. For dilute solutions of long thin rods the diffusion constants are $D_\perp = D_\parallel/2 = D/2$ and $D_r = 6D/l^2$, with $D = k_B T \ln(l/b)/(2\pi\eta l)$ and η the solvent viscosity [14]. In this regime the instability of the homogeneous solution occurs at $\tilde{\alpha}^{(1)}_c$ and is associated with the density mode.

Semi-dilute Solutions. For semidilute solutions, the dynamics is modified by the topological constraint that the filaments cannot pass through each other. This constraint can be modeled by a tube [14, 16] leading to modified transverse and rotational diffusivities, $D_\perp \simeq D/[2(1 + c_\perp \tilde{\rho}_0 (l/b)^{d-2})^2]$ and $D_r \simeq 6D/[l^2(1 + c_r \tilde{\rho}_0 (l/b)^{d-2})^2]$ with $c_{r,\perp}$ numbers of order unity and $D_\parallel$

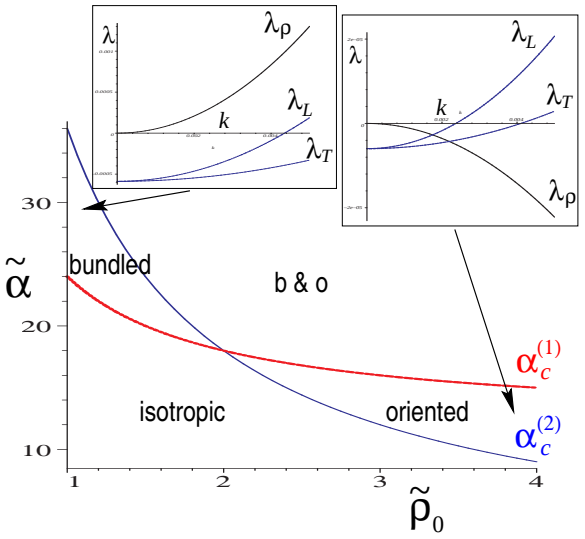

FIG. 2: Linear modes and phase diagram $\{\tilde{\alpha}, \tilde{\rho}_0\}$ showing the phase boundaries $\alpha_c^{(1)}, \alpha_c^{(2)}$ between the homogeneous state and the density and orientationally inhomogeneous state. The modes on the right corresponds to $\alpha l/D = 10, \tilde{\rho}_0 = 10, l/b = 100$ while those on the left $\alpha l/D = 1900, \tilde{\rho}_0 = 1, l/b = 100$.

essentially unaffected by entanglement [14, 16]. The kinetic modes λ_- and λ_T describing the decay of orientation fluctuations can then become unstable before the density mode. This instability occurs at $\tilde{\alpha}_c^{(2)} \approx 1/\tilde{\rho}_0$ for $k > k_0$, with $k_0 \simeq (1/l\tilde{\rho}_0)\sqrt{\frac{d(d+2)}{3(\tilde{\alpha}\tilde{\rho}_0 - d)}}$. A stability diagram in the $(\tilde{\alpha}, \tilde{\rho}_0)$ plane is shown in Fig. 2.

Semiflexibility. Semiflexible filaments of persistence length $\ell_p > l$ can be modeled as fuzzy rods with a diameter given by $b \equiv \sqrt{l^3/\ell_p}$ leading to $v_0 = l^{2+3(d-2)/2}\ell_p^{-(d-2)/2}$.

Discussion. The linear instability of the homogeneous state is controlled by the parameter α that drives filament bunching, while β and γ play no role [17]. At low filament densities, well below the critical density for the nematic transition, density fluctuations become unstable on all length scales at $\alpha_c^{(1)}$, signaling the onset of a state with inhomogeneous density. For $\tilde{\rho}_0 > \tilde{\rho}_c \simeq 2$, where the critical curves $\alpha_c^{(1)}$ and $\alpha_c^{(2)}$ cross, the instability occurs at the lower value $\alpha_c^{(2)}$ and it corresponds to a short-scale instability of orientation fluctuations, while the density remains homogeneous. In this regime the filament solution has a substantial degree of short range nematic order and both transverse and rotational diffusion are strongly impeded. The orientational degree of freedom, $\mathbf{t}$, becomes essentially conserved as D_r is vanishingly small. The mechanism for the orientational instability of dense filament solutions obtained here is distinct from that proposed by Lee and Kardar [11]. These authors modeled the dynamic in the nematic phase and incorporated an inhomogeneous motor density. In their model the instability is controlled by the nonlinear coupling of orientation to motor density fluctuations. Here, in contrast the instability occurs to linear order and is driven by the pattern-forming terms in Eq. (12).

A number of open questions remain. It will be relatively straightforward to include the motor transport using our formalism. This is important for very processive motors and at low motor densities. An inhomogeneous motor density may also be required for the formation of stable asters and vortices at low filament concentration. It will be also very interesting to ask about the response of the motor/filament system to shear. This work will be presented elsewhere [18].

We thank E. Frey, K. Kruse, F. MacKintosh, A.C. Maggs, D. Morse and S. Ramaswamy for many helpful discussions. This research was supported in part by the National Science Foundation under Grants No. PHY99-07949 (at KITP), DMR97-30678 (at Syracuse) and the Royal Society (London).

[1] J. Howard, *Mechanics of Motor Proteins and the Cytoskeleton*, (Sinauer, New York, 2000).
[2] L. Le Goff, F. Amblard and E. Furst, *Phys. Rev. Lett.*, **88**, 018101 (2002)
[3] D. Humphrey, C. Duggan, D. Saha, D. Smith and J. Käs, *Nature* **416**, 413 - 416 (2002).
[4] F. J. Nédélec, T. Surrey, A. C. Maggs and S. Leibler, Nature **389**, 305 (1997).
[5] T. Surrey, F. J. Nédélec, S. Leibler and E. Karsenti, Science **292**, 1167 (2001).
[6] M. Dogterom, A. C. Maggs and S. Leibler, Proc. Nat. Acad. Sci. USA **92**, 6683 (1995).
[7] Pattern formation in cells is of course regulated by complex biochemical reaction networks. Here we focus only on the underlying physical processes.
[8] H. Nakazawa and K. Sekimoto, J. Phys. Soc. Jpn. **65** 2404 (1996); K. Sekimoto and H. Nakazawa, in *Current Topics in Physics*, Y. M. Cho, J B. Homg and C. N. Yang, eds. (World Scientific, Singapore, 1998).
[9] B. Bassetti, M. C. Lagomarsino and P. Jona, Eur. Phys. J. B **15**, 483 (2000).
[10] K. Kruse and F. Jülicher, Phys. Rev. Lett. **85**, 1779 (2000); *ibidem* cond-mat/0207212.
[11] H. Y. Lee and M. Kardar, Phys. Rev. E **64**, 56113 (2001).
[12] K. Kruse, S. Camalet and F. Jülicher, Phys. Rev. Lett. **87**, 138101 (2001).
[13] D. Humphrey, C. Duggan, D. Saha, D. Smith and J. Käs, *unpublished.*
[14] M. Doi and S. F. Edwards, *The theory of polymer dynamics*, Oxford University Press (New York, 1986).
[15] The full nonlinear equations can be found at http://physics.syr.edu/˜mcm/nonlinear_eqs.pdf
[16] I. Teraoka and R. Hayakawa, *J. Chem. Phys.* **89**, 6989 (1988); *J. Chem. Phys.* **91**, 2643 (1989).
[17] β controls, however, the length scale at which the modes are stabilized at higher wavevectors.
[18] T.B. Liverpool and M.C. Marchetti, *unpublished.*